Journal of Chromatography B, 913–914 (2013) 106–112

Contents lists available at SciVerse ScienceDirect

Journal of Chromatography B

journal homepage: www.elsevier.com/locate/chromb

# *In chemico* evaluation of skin metabolism: Investigation of eugenol and isoeugenol by electrochemistry coupled to liquid chromatography and mass spectrometry

Daniel Melles[a], Torsten Vielhaber[a], Anne Baumann[a], Raniero Zazzeroni[b], Uwe Karst[a,*]

[a] *Westfälische Wilhelms-Universität Münster, Institut für Anorganische und Analytische Chemie, Corrensstraße 30, 48149 Münster, Germany*
[b] *Unilever U.K., Safety & Environmental Assurance Centre, Colworth Science Park, Sharnbrook, Bedfordshire MK 44 1LQ, United Kingdom*

ARTICLE INFO

*Article history:*
Received 26 September 2012
Accepted 4 December 2012
Available online 11 December 2012

*Keywords:*
Electrochemistry
Eugenol
Isoeugenol
Metabolism
Protein modification

ABSTRACT

Skin sensitization is initiated by the modification of proteins located in the skin. After oxidative activation, eugenol and isoeugenol have the potential to modify skin proteins and therefore cause sensitization processes. Despite their known skin sensitizing properties, they are of common use in cosmetic products. According to the European Commission regulation No. 1223/2009, animal tests have to be banned for substances intended for cosmetic use. Therefore, alternative methods of investigation need to be developed for the approval of future substances. For this reason, eugenol and isoeugenol were selected as model substances to be investigated in a purely instrumental approach comprising electrochemistry, liquid chromatography and mass spectrometry. In the present work, reactive oxidation products of eugenol and isoeugenol were electrochemically generated. Reactive quinones and quinone methides were formed. Surprisingly, eugenol and isoeugenol differ significantly in their oxidation behaviour. Isoeugenol exhibits the formation of quinones and quinone methides of an alkylated and dealkylated species, respectively, whereas eugenol shows the formation of quinoid species only after dealkylation. Reactive quinoid species could be trapped with glutathione and the protein β-lactoglobulin A. The results are comparable to the ones with conventional animal studies in literature, which attribute the adverse effects of eugenol and isoeugenol to the formation of reactive quinones or quinone methides, which are reactive intermediates, able to react with proteins. Such species were successfully generated and investigated by the use of electrochemistry coupled to mass spectrometry. Above all, the investigation of adduct formation by the additional use of liquid chromatography allowed the assessment of the mechanism of oxidation, as it might happen in the skin. Both substances were proven to be trapped by the protein β-lactoglobulin A after electrochemical oxidation. However, isoeugenol formed the larger variety of adducts compared to eugenol.



## 1. Introduction

Eugenol and isoeugenol are fragrances commonly used in a variety of products, including cosmetics, although these substances have been reported to cause skin sensitizing effects in several studies [1–4]. The process of skin sensitization involves a complex sequence of events. However, certain key steps have been identified so far. First, a skin sensitizing agent has to penetrate the skin, in which skin inherent proteins can be modified either by this agent or one of its metabolites. Subsequently, the formed complex is processed by different specialized cell types, which finally induce an activation of the body's own defence system. An inflammation of the skin can consequently be observed after re-exposure to the reactive species [5–8]. A crucial step in this process is the modification of the protein, as it represents the initialization of the sensitization process. A number of compounds are referred to as skin sensitizers, although their structures bear no reactive groups, prone to react with functional groups in proteins. These substances have to undergo an activation process before protein modification may occur [9,10]. In this case, the compound is usually oxidized to the attributed reactive structure. A lot of compounds such as p-phenylendiamine, d-limonene, linalool and urushiols, just to mention a few, have been proven to show their skin sensitizing effect exclusively after oxidative activation [11–15]. The skin is not known to favour oxidative biotransformation, although the respective preconditions do exist. The oxidation is thought to take place both in pure chemical processes including autoxidation and in enzymatic reactions. Typically, oxidative enzymatic alterations in the skin are ascribed to the enzyme group of cytochrome P450 (CYP450) [16–18], but

* Corresponding author. Tel.: +49 251 8333141; fax: +49 251 8336013.
*E-mail address:* uk@uni-muenster.de (U. Karst).

1570-0232/$ – see front matter © 2012 Elsevier B.V. All rights reserved.
http://dx.doi.org/10.1016/j.jchromb.2012.12.004

alcohol deydrogenases, aldehyde dehydrogenases [19] and flavin-containing monooxygenases [20] may be involved as well. For example, the oxidation of eugenol and isoeugenol has been allocated to the activity of CYP450 enzymes [21]. According to studies on structural properties and their correlation to skin sensitization, catechols and hydroquinones cause skin sensitization due to the formation of reactive *o*-quinones or *p*-quinones, respectively. Similar activation processes are described for eugenol and isoeugenol. Eugenol is likely to exhibit an *O*-dealkylation followed by the formation of an *o*-quinone and/or a *p*-quinone methide. Isoeugenol can also undergo the formation of a quinone methide without previous dealkylation [21,22]. Investigations on eugenol with liver microsomes, a commonly used tool for studies on the oxidative metabolism, also confirm the formation of quinoid structures, although the applicability of these studies did not cover the skin sensitization potential of this compound. Eugenol has also been shown to be oxidized to the attributed alkylated quinone methide [23].

In recent years, various studies on the mimicry of these oxidation reactions by the use of electrochemistry coupled to mass spectrometry (EC/MS) or even to liquid chromatography and mass spectrometry (EC/LC/MS) have been conducted, demonstrating that this setup has the ability to be a complementary tool in metabolic investigations [24–29]. The oxidative metabolism of paracetamol and amodiaquine could readily be mimicked [30,31]. This method presents the advantage that oxidation products can be investigated instantly after generation so that very reactive oxidation products with short half-life times can be generated and detected before any rearrangement or reaction with other species. Lately, several papers reviewed the use of electrochemistry in metabolic studies [32–35]. An extension of this approach by the use of proteins has been achieved by Lohmann et al. The drugs paracetamol, amodiaquine and clozapine were electrochemically oxidized and corresponding products were trapped with a protein, which was subsequently analysed by LC/MS [36].

So far, few skin sensitization tests focus on a mechanistic understanding of the compound and its behaviour in skin. Therefore, our aim is to achieve the oxidative activation and subsequent protein modification by the use of EC/MS and EC/LC/MS. Above all, the motivation in this project is based on the properties and future perspectives of the electrochemical approach. Not only the instant detection of reactive species, but also the avoidance of complex biological matrices in the investigation of adducts provides a comprehensive overview of possible adverse reactions. Thus, electrochemistry may have the potential to become an additional tool in the investigation of skin sensitizers, in particular with respect to EU regulations, which ban the use of animal tests in the admittance of cosmetic substances and will be in full effect in 2013. Our respective work about the skin sensitizers eugenol and isoeugenol is presented within this manuscript.

## 2. Experimental

### 2.1. Chemicals

Eugenol, isoeugenol, β-lactoglobulin A (β-LGA), glutathione (GSH), ammonium acetate, formic acid and guanidine hydrochloride were purchased from Sigma–Aldrich Chemie GmbH (Steinheim, Germany). Acetonitrile was obtained from Merck (Darmstadt, Germany). Water for sample preparation and chromatography was purified with an Aquatron A4000D system (Barloworld Scientific, Nemours Cedex, France) prior to use.

### 2.2. Instrumentation

The device used for the generation of oxidation products consisted of an amperometric thin-layer cell (Flex Cell®, Antec Leyden, Zoeterwoude, The Netherlands) controlled by either a Roxy potentiostat (Antec Leyden) or a homemade device. All electrochemical oxidations were conducted on boron doped diamond (BDD) working electrodes with $Pd/H_2$ as reference electrode.

The LC system used in this work was from Antec Leyden and comprised two LC 100 pumps, an OR 110 organizer rack with a degasser and a pulse dampener, an AS 100 autosampler and a Roxy potentiostat and column oven. MS analyses were performed on a micrOTOF mass spectrometer from Bruker Daltonics (Bremen, Germany) equipped with an electrospray ionization (ESI) source.

### 2.3. Mass voltammograms

Mass voltammograms of eugenol and isoeugenol were recorded by online coupling of the electrochemical cell to the ESI interface of the mass spectrometer by a transfer capillary (EC/MS). A 50 μM solution of either eugenol or isoeugenol in a mixture of 1 mM ammonium acetate (pH 7.4) and acetonitrile (50/50, v/v) was pumped through the cell at a flow rate of 10 μL/min by a syringe pump model 74900 (Cole Parmer, Vernon Hills, IL, USA). The effluent was transferred into the ESI interface of the MS. The potential was gradually increased from 0 to 2500 mV *vs.* $Pd/H_2$ at a scan rate of 10 mV/s. Mass spectra were recorded in negative ion mode applying following conditions: nebulizer ($N_2$): 0.6 bar; dry gas ($N_2$): 3.5 L/min; dry heater: 200 °C; capillary: 4.5 kV; endplate offset: −500 V; capillary exit: −105 V; skimmer 1: −35 V; skimmer 2: −25.5 V; hexapole 1: −28.5 V; hexapole RF: 112.5 V; lens transfer time: 40 μs; pre pulse storage time: 5 μs; lens 1 storage: −30 V; lens 1 extraction: −20.8 V; lens 2: −8.4 V; lens 3: 20.8 V; lens 4: −0.3 V; lens 5: 27.5 V; mass to charge (*m*/*z*) ratio range: 50–500 *m*/*z*.

Mass voltammograms were also generated for trapping experiments with GSH. The electrochemical oxidation of eugenol or isoeugenol was performed under the conditions mentioned above. After the electrochemical oxidation, the effluent was mixed online with a 25 μM aqueous solution of GSH in 1 mM ammonium acetate (pH 7.4) via a T-piece. The GSH-containing solution was continuously added at a flow rate of 10 μL/min, resulting in a total flow of 20 μL/min for the mixed solution. The mixture was allowed to react for 2 min inside the transfer capillary (PEEK, length: 20.4 cm, i.d.: 0.5 mm) before reaching the ESI interface of the mass spectrometer. The conditions for the MS were modified as follows, capillary exit: 135 V; skimmer 1: −45 V; skimmer 2: −25.5 V; hexapole 1: −25.5 V; hexapole RF: 150 V; lens transfer time: 50 μs; pre pulse storage time: 1.2 μs; lens 1 extraction: −21.8 V; mass to charge (*m*/*z*) ratio range: 50–1000 *m*/*z*.

### 2.4. Adduct formation using proteins

A 100 μM solution of either eugenol or isoeugenol in 1 mM ammonium acetate (pH 7.4) and acetonitrile (50/50, v/v) was pumped through the electrochemical cell at a constant potential of 2000 mV and flow rate of 10 μL/min. The effluent of the cell was mixed with β-LGA solution (20 μM in 6 M aqueous guanidine hydrochloride) via a T-piece. The mixture was pumped through a reaction coil (PEEK, length: 102 cm cm, i.d.: 0.5 mm) for 10 min and was collected in a 20 μL injection loop mounted on a 10-port switching valve. The sample was flushed onto the column by switching the valve. Acetonitrile and 0.1% formic acid (pH 2.6) were used as mobile phases on a Discovery BIO Wide Pore C5 column (2.1 mm × 150 mm, particle size 5 μm) from Supelco (Bellefonte, PA, USA). The separation was performed at a constant flow rate of

**Table 1**
Gradient profile used for the clean-up of protein adducts.

| Time (min) | 0 | 2 | 6 | 9 | 12 | 15 |
|---|---|---|---|---|---|---|
| Acetonitrile (%) | 25 | 25 | 70 | 70 | 25 | 25 |

300 μL/min and the temperature was kept at 40 °C. The gradient profile is shown in Table 1. Mass spectra were recorded in positive ion mode: nebulizer ($N_2$): 1.8 bar; dry gas ($N_2$): 8.0 L/min; dry heater: 190 °C; capillary: −4.0 kV; endplate offset: −300 V; capillary exit: 180 V; skimmer 1: 60 V; skimmer 2: 25.0 V; hexapole 1: 23.0 V; hexapole RF: 300.0 V; lens transfer time: 70 μs; pre pulse storage time: 25 μs; lens 1 storage: 30 V; lens 1 extraction: 21.3 V; lens 2: 7.4 V; lens 3: 21.0 V; lens 4: 0.3 V; lens 5: −27.5 V; mass to charge (*m*/*z*) ratio range: 50–4000 *m*/*z*.

## 3. Results and discussion

### 3.1. Mass voltammograms of eugenol and isoeugenol

By applying a potential ramp of 0–2500 mV and recording mass spectra in defined time intervals, oxidation products of eugenol and isoeugenol were identified in mass voltammograms: plotting the mass spectra *vs.* the applied potential allows the identification of potential oxidation products by increasing signal intensities. The mass voltammograms for eugenol and isoeugenol are presented in Fig. 1. As shown in Fig. 1a, the signal of the parent substance eugenol with *m*/*z* 163 decreases with increasing potential. The highest signal intensity was observed for the oxidation product at *m*/*z* 149. This finding is in accordance with an *O*-demethylation reaction

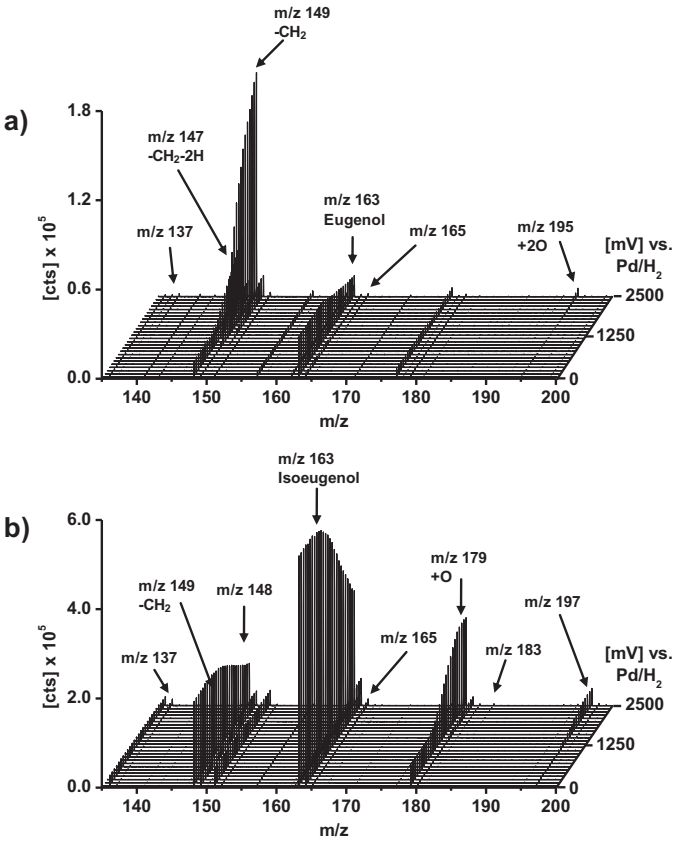


**Fig. 1.** 3D plot (mass voltammogram) of (a) eugenol and (b) isoeugenol, generated in an EC/ESI-ToF/MS-system operating in ESI(−) mode. The signal intensity is plotted against the mass-to-charge ratio (*m*/*z*, *x*-axis) and the applied cell potential (0–2500 mV, *z*-axis).

(−$CH_3$) of eugenol, leading to the formation of a second hydroxyl group in the product *m*/*z* 149, which can be readily deprotonated in the negative ion mode. Comparing the signal intensity of *m*/*z* 149 to the signal intensity of eugenol reveals that the response of *m*/*z* 149 in (−)ESI-MS detection is significantly higher due to enhanced ionization properties. The product *m*/*z* 147 is expected to be an oxidation product of *m*/*z* 149, originating from a dehydrogenation reaction. Consequently, this leads to the formation of the corresponding *o*-quinone or quinone methide of the dealkylated product (*m*/*z* 149, Fig. 2). Further products formed upon oxidation are *m*/*z* 137, 165 and 195. According to the mass gain of +32 from the parent substance eugenol (*m*/*z* 163), the product *m*/*z* 195 is attributed to a formal addition of two oxygen atoms. The *m*/*z* ratios 137 and 165 presumably derive from the dealkylated product (*m*/*z* 149) with *m*/*z* 165 resulting from the addition of one oxygen atom to *m*/*z* 149. Details for the oxidation process of eugenol are discussed in detail in Fig. 2.

Isoeugenol is electrochemically active and forms different oxidation products from eugenol, as can be seen from Fig. 1b. Comparing the mass voltammograms of eugenol (Fig. 1a) and isoeugenol (Fig. 1b) reveals that the response of the parent substance isoeugenol in (−)ESI-MS detection is much higher than for eugenol, which is presumably due to the fact that the double bond in the side chain of isoeugenol is conjugated with the aromatic moiety. Provided that ionization takes place at the hydroxyl group, the negative charge can thus be better delocalized compared to eugenol. Additionally, another decreasing signal with *m*/*z* 148 was observed. It is likely to be a fragment of isoeugenol with *m*/*z* 163, as it is already present at 0 mV and decreases in parallel to the parent isoeugenol. The ion *m*/*z* 179 is the most dominant product and is likely to be formed via a hydroxylation reaction, which presumably occurs at the aromatic moiety or at the double bond in the side chain. Signals related to eugenol are also found for *m*/*z* 137, 149 and 165. These adducts are similar to those of eugenol. The product *m*/*z* 149 is formed under dealkylation of the parent isoeugenol, whereas *m*/*z* 137 and 165 represent further products of *m*/*z* 149. Furthermore, two products with *m*/*z* 183 and 197 were identified, which were not observed for eugenol. They are suspected to be subsequent products from the oxidation of the dealkylated product *m*/*z* 149. It is interesting that isoeugenol demonstrates a larger product range than eugenol, although the only difference between both structures is the position of the double bond in the side chain.

Exact masses were determined to confirm the molecular formulas of the stated products and are presented in Table 2. For the oxidation of eugenol, the observed masses are in good agreement with the calculated masses, as illustrated in Table 2a. Only *m*/*z* 137 and 165 show a mass deviation of 5 ppm or slightly higher, but these signals are low in intensity and the mass deviation can be

**Table 2**
Determined masses and corresponding proposals for molecular formulae of oxidation products of eugenol and isoeugenol.

| Measured *m*/*z* | Calculated *m*/*z* | Deviation [ppm] | Molecular formula |
|---|---|---|---|
| Eugenol | | | |
| 137.0238 | 137.0244 | 4.8 | $C_7H_5O_3$ |
| 147.0449 | 147.0452 | 1.7 | $C_9H_7O_2$ |
| 149.0605 | 149.0608 | 2.0 | $C_9H_9O_2$ |
| 165.0565 | 165.0557 | 4.7 | $C_9H_9O_3$ |
| 195.0656 | 195.0655 | 3.6 | $C_{10}H_{11}O_4$ |
| Isoeugenol | | | |
| 137.0245 | 137.0244 | 0.2 | $C_7H_5O_3$ |
| 147.0459 | 147.0452 | 5.2 | $C_9H_7O_2$ |
| 149.0591 | 149.0608 | 11.3 | $C_9H_9O_2$ |
| 165.0579 | 165.0557 | 13.4 | $C_9H_9O_3$ |
| 179.0710 | 179.0714 | 1.9 | $C_{10}H_{11}O_3$ |
| 183.0642 | 183.0663 | 11.6 | $C_9H_{11}O_4$ |
| 197.0816 | 197.0819 | 1.7 | $C_{10}H_{13}O_4$ |

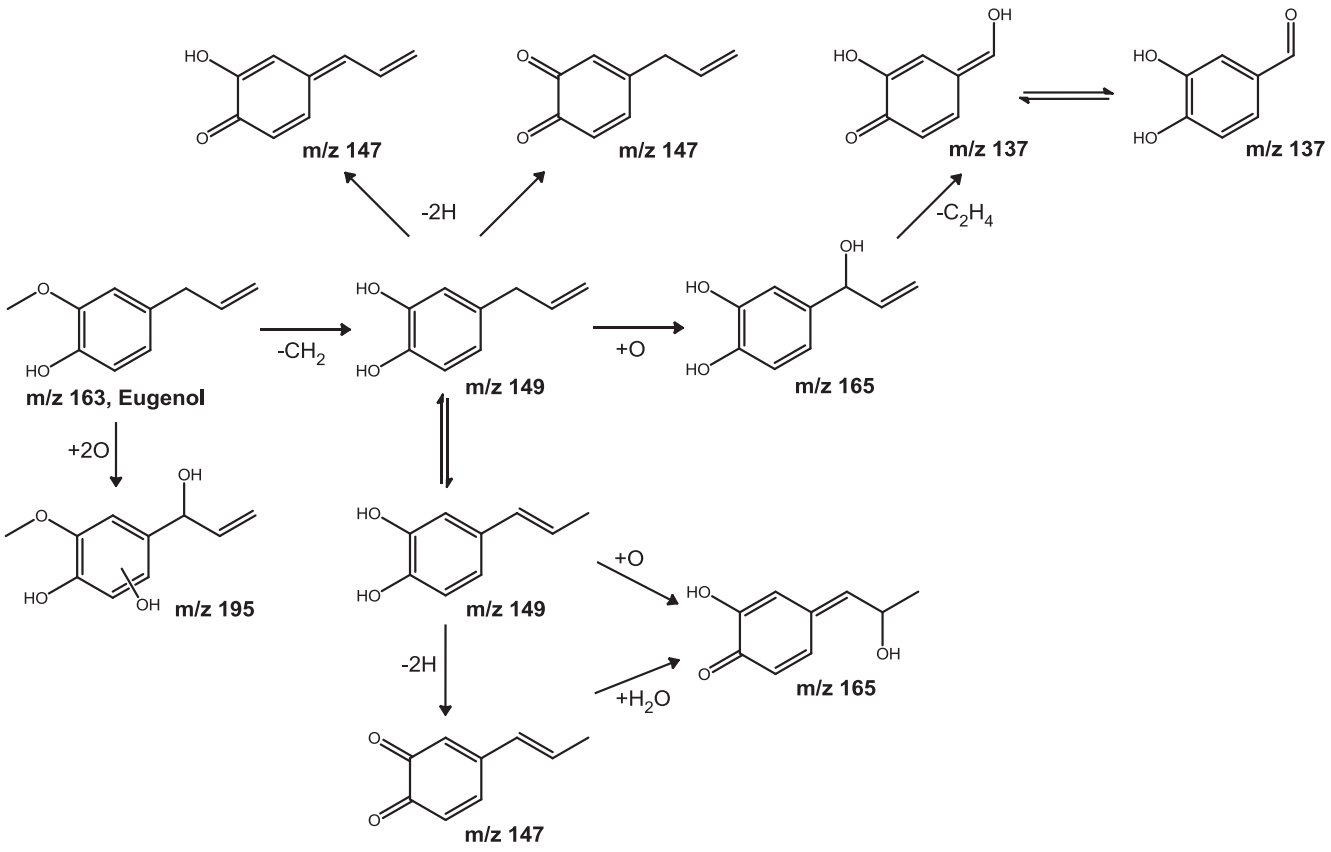


**Fig. 2.** Proposed oxidative pathway of eugenol.

affected by overlying interfering masses. Calculations carried out for isoeugenol are presented in Table 2b. In contrast to the results obtained for eugenol, some products exhibit relatively high mass deviations. The deviation of 11.3 ppm between the calculated and measured mass for *m*/*z* 149 results from the overlap with the isotope pattern of *m*/*z* 148. This is the case for *m*/*z* 165 as well, which interferes with the isotope pattern of the parent isoeugenol (*m*/*z* 163). There is no direct interference for the mass 183, but as it is detected at very low intensity, it is likely to be affected by interfering background.

Based on exact masses of the oxidation products and resulting molecular formulas, oxidation pathways were deduced for both eugenol and isoeugenol. Fig. 2 depicts the oxidation pathway of eugenol. Starting at eugenol (*m*/*z* 163), an *O*-demethylation takes place (*m*/*z* 149), which is followed by the formation of a quinone or quinone methide species (*m*/*z* 147). The product *m*/*z* 165 correlates with a demethylation reaction in combination with an oxygenation reaction. Presumably, the product is formed via an oxygenation of the demethylation product *m*/*z* 149. This is supported by the fact that *m*/*z* 165 is formed at higher potentials than *m*/*z* 149. The oxygenation is likely to take place at the allylic/benzylic position or at the aromatic moiety. A direct oxygenation at the former double bond may also occur. The product *m*/*z* 195 reveals the gain of two oxygen atoms, most likely resulting from a hydroxylation at the aromatic moiety and at the allylic/benzylic position. It was surprising that there was no singly oxygenated species occurring upon oxidation (*m*/*z* 179). Hence, it is assumed that this intermediate was directly transformed into *m*/*z* 195. For *m*/*z* 137, two different structures are postulated. It is likely that an *O*-demethylation reaction and the oxidative degradation of the side chain take place.

Fig. 3 shows a proposal for the main oxidation path of isoeugenol. Herein, the main oxidation product *m*/*z* 179 results from a hydroxylation reaction occurring at the aromatic moiety or at the double bond in the side chain. As indicated, a reactive quinone methide structure is expected to be formed. The product *m*/*z* 165 reveals that an *O*-dealkylation reaction takes place, in combination with a hydroxylation, as it was already observed for eugenol. Again, the hydroxylation occurs at the aromatic moiety or the double bond in the side chain. The structures presented for the products *m*/*z* 183 and 197 demonstrate that doubly and triply oxygenated *O*-dealkylation products were formed. The proposed structure for *m*/*z* 183 unveils the formation of a diol from the former double bond. This reaction presumably proceeds via the *O*-dealkylated and hydroxylated product *m*/*z* 165. The product *m*/*z* 137 shows the loss of the side chain of isoeugenol. The oxidation pathway of isoeugenol shows that different *O*-demethylated and hydroxylated species are formed. Similarly as for eugenol, the dealkylated product *m*/*z* 149 and the corresponding product *m*/*z* 147 are observed. However, multiply hydroxylated *O*-demethylation products were identified, which did not occur upon oxidation of eugenol. Hence, the results indicate that isoeugenol is more readily hydroxylated than eugenol. Nevertheless, the structure elucidation using fragmentation by $MS^n$-experiments gave no characteristic hints to the formed oxidation products.

Since different quinones or quinone methides appear in the oxidation pathway of both eugenol and isoeugenol, it is likely that adduct formation with nucleophilic species takes place in the organism. Therefore, the ability to react with GSH has been investigated. The adduct formation was monitored and plotted in mass voltammograms. The oxidized solution of eugenol or isoeugenol was mixed with a GSH solution. The mixture was then allowed to react for 2 min and was analysed by ESI-ToF-MS. Adducts were identified by their increasing signal intensity. Fig. 4a shows the obtained 3D plot, which clearly indicates the formation of a glutathione adduct with an oxidation product of eugenol above

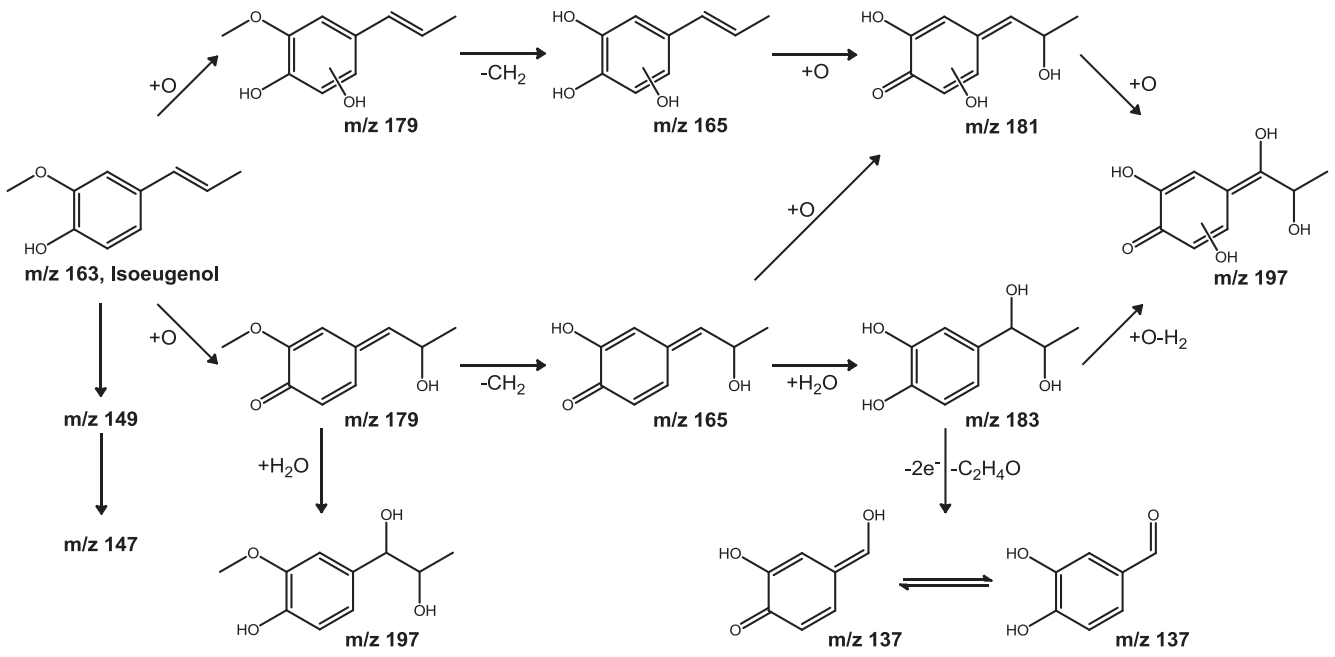


**Fig. 3.** Proposed oxidative pathway of isoeugenol.

1200 mV (*m*/*z* 454). The signals *m*/*z* 476 and 498 are the corresponding sodium adducts, bearing one and two sodium ions, respectively. This result is in accordance with the assumption that GSH traps soft electrophiles such as quinones or quinone methides, such as the oxidation product *m*/*z* 147 of eugenol. The reaction between the product *m*/*z* 147 and GSH leads to an adduct with *m*/*z* 454, following a Michael addition mechanism. The corresponding molecular formula $C_{19}H_{24}N_3O_8S_1$ (calculated *m*/*z*: 454.1290, determined *m*/*z*: 454.1274) in negative ion mode was detected with a deviation of 3.4 ppm. Fig. 4b shows an increased variety of adducts obtained with isoeugenol. The adduct at *m*/*z* 454 was generated and identified as an adduct formed between the *O*-demethylation product of isoeugenol and GSH. An associated sodium adduct *m*/*z* 476 was also observed. Yet, additional adducts (*m*/*z* 470, 486, 488 and 492) were observed, indicating a higher reactivity of the oxidation products of isoeugenol towards GSH. The adduct *m*/*z* 470 presumably represents the adduct formation between the oxidation product *m*/*z* 165 and GSH, resulting in the molecular formula $C_{19}H_{24}N_3O_9S_1$ (calculated *m*/*z*: 470.1239, determined *m*/*z*: 470.1223) in negative ion mode, which was observed with a deviation of 3.3 ppm. Replacement of hydrogen with sodium would lead to a mass 492, which was also found. The product *m*/*z* 486 is presumably formed between the main oxidation product *m*/*z* 179 (isoeugenol + O) and GSH. Again, a quinone or quinone methide is the reactive intermediate. The expected molecular formula $C_{20}H_{28}N_3O_9S_1$ (calculated *m*/*z*: 486.1552, determined *m*/*z*: 486.1530) is confirmed by a mass deviation of 4.4 ppm. Finally, the adduct *m*/*z* 488 has been identified, and the determined molecular formula $C_{19}H_{26}N_3O_{10}S_1$ (calculated *m*/*z*: 488.1344, determined *m*/*z*: 488.1328) correlates to an adduct formed between the oxidation product *m*/*z* 183 and GSH with a mass deviation of 3.3 ppm.

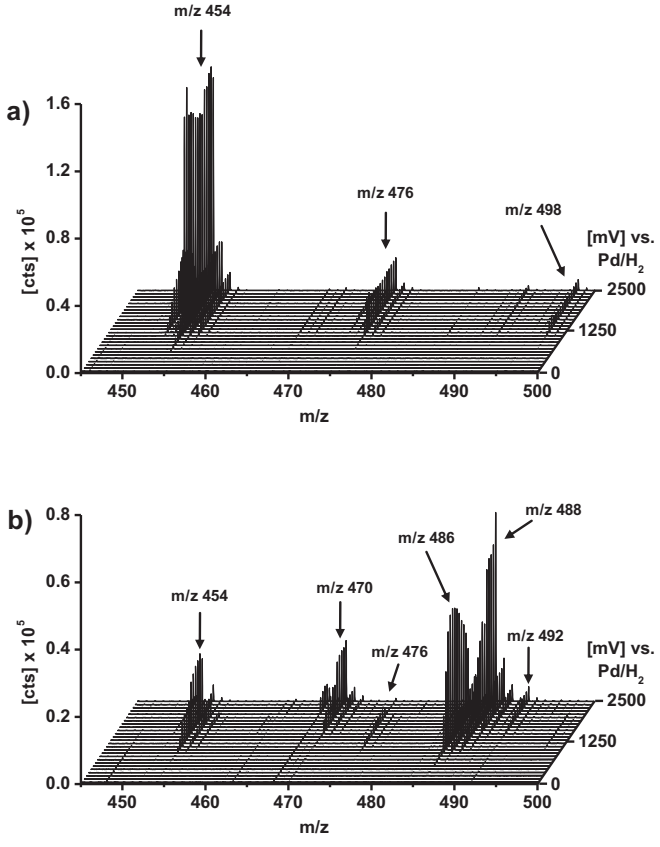


**Fig. 4.** Mass voltammogram of (a) eugenol and (b) isoeugenol after online addition of the trapping agent GSH.

### 3.2. Adduct formation using proteins

To demonstrate the reactivity of the oxidation products of eugenol and isoeugenol with proteins, an instrumental approach with the model protein β-LGA was established, as this protein is characterized by a comparably low mass (18,363 Da) and is structurally homogeneous. It contains one free thiol group and is thus a potential target for electrophiles. The results for the adduct formation between the protein and eugenol or isoeugenol are presented in Fig. 5. In a first experiment, a blank test without eugenol or isoeugenol was conducted, which is shown in Fig. 5a. The ESI-MS spectrum with different charge states was deconvoluted to obtain the corresponding neutral mass of the protein (18,363 Da). Fig. 5b presents the results of the adduct formation with an

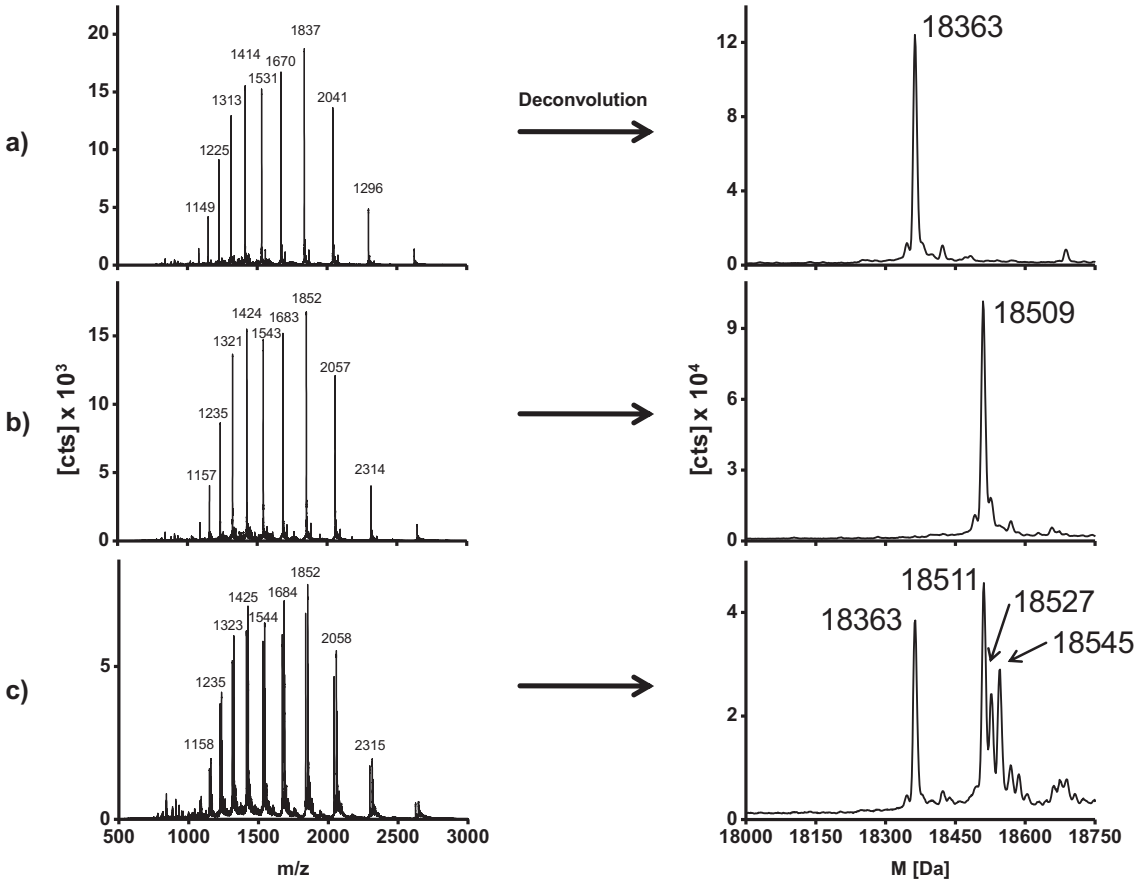


**Fig. 5.** Adduct formation of β-LGA with reactive oxidation products of eugenol and isoeugenol, generated at a constant potential of 2000 mV: (a) oxidation of a blank solution and subsequent addition of β-LGA, (b) oxidized eugenol and subsequent addition of β-LGA, (c) oxidized isoeugenol and subsequent addition of β-LGA. Raw ESI-ToF/MS spectra of the protein are depicted in the left column, corresponding deconvoluted neutral mass spectra are depicted in the right column.

electrochemically treated (2000 mV) solution of eugenol. Agreeing with the results obtained for GSH, one major adduct is formed with a mass of 18,509 Da. The mass gain to the non-modified β-LGA is in good accordance with the addition of the oxidation product *m*/*z* 147, which is the quinone/quinone methide shown in Fig. 2. The same oxidation product has been identified to react with GSH (see previous chapter/mass voltammograms). As can be seen from the deconvoluted mass spectra in Fig. 5c, three different protein adducts are formed in case of the oxidation of isoeugenol. The adduct with a neutral mass of 18,511 Da correlates to the adduct formation between the oxidation product *m*/*z* 147 and β-LGA. This product has previously been identified to form an adduct with GSH (*m*/*z* 454). The protein adduct with the mass 18,527 Da shows a difference to the non-modified protein of 164 Da, which is in good agreement with the oxidation product *m*/*z* 165. The same electrochemical product has been shown to form a GSH adduct (*m*/*z* 470). The third protein adduct (18,545 Da) reveals a difference of 183 Da to the non-modified protein. Hence adduct formation has taken place between β-LGA and the oxidation product *m*/*z* 183. A respective GSH adduct has been identified at a *m*/*z* ratio of 488.

## 4. Conclusions

As can be concluded from the recorded mass voltammograms (Fig. 1), both eugenol and isoeugenol are active upon electrochemical oxidation. Although similar in structure, the oxidation pathways differ strongly from each other. Both compounds show the formation of *O*-demethylated products and related secondary products. However, isoeugenol additionally reveals the generation of oxygenated products without previous demethylation. Adduct formation is a crucial step in the assessment of potent skin sensitizers, since the sensitization process is initiated by the modification of skin inherent proteins. First, the adduct formation was investigated by the use of the strongly nucleophilic tripeptide glutathione, which is the major low molecular weight thiol present in animal cells and plays an important role in detoxification. Glutathione is a frequently used surrogate for the reactivity towards proteins. The oxidation products of both eugenol and isoeugenol were successfully trapped by glutathione, whereby isoeugenol forms a wider variety of adducts. Glutathione is a frequently used surrogate for the reactivity towards proteins. Finally, a comprehensive investigation involving protein trapping experiments with β-lactogloublin A was carried out. Again, the results demonstrate that the oxidation products of eugenol and isoeugenol are potent agents able to react with proteins. Herein, isoeugenol shows the formation of two additional adducts, which are in agreement with the findings made with glutathione. These trapping experiments lead to the conclusion that isoeugenol apparently forms more reactive products towards glutathione and β-LGA upon electrochemical oxidation. Comparing these results with previously conducted *in vivo* and *in vitro* studies on the skin sensitizing properties, the results presented here are largely in agreement with literature data. The adverse side effects of both substances are thought to be caused by the formation of electrophilic structures such as quinones or quinone methides and these structures were also found within the present work. Additionally, isoeugenol turned out to form more species, which

are reactive towards glutathione and proteins. This may underline the observation that isoeugenol is a more potent sensitizer than eugenol. Therefore, the approach using the hyphenation of electrochemistry, liquid chromatography and mass spectrometry may have the potential to serve as a complementary tool in the assessment of skin sensitizers. Oxidative activation in the skin is supposed to be caused by several mechanisms. As a result, an ideal test for skin sensitization should include the possibility to evaluate the entire potential for a chemical to react. Hence, the purely instrumental EC/LC/MS approach is a technique for the screening of cosmetic ingredients towards their ability to form electrochemical-induced oxidation products and furthermore, to screen the reactivity of the oxidation product towards nucleophiles such as GSH or proteins. However, the correlation to clinical symptoms cannot easily be answered with this method, as the focus is on the initial, often cost and time consuming, screening of new ingredients. Future investigations will be focused on EC/LC/NMR/MS experiments to elucidate the purified formed metabolites in more detail. Based on this initial work, several other proteins such as human serum albumin and haemoglobin are supposed to be evaluated towards adduct formation with electrochemically generated metabolites of eugenol, isoeugenol and other chemicals.

## Acknowledgements

This study was supported in part by the Deutsche Forschungsgemeinschaft (Bonn, Germany), the Fonds der Chemischen Industrie (Frankfurt am Main, Germany) and the Graduate School of Chemistry (Münster, Germany).

## References

[1] D.A. Basketter, K.E. Andersen, C. Liden, H. Van Loveren, A. Boman, I. Kimber, K. Alanko, E. Berggren, Contact Dermatitis 52 (2005) 39.
[2] C.D. Calnan, E. Cronin, R.J. Rycroft, Contact Dermatitis 6 (1980) 500.
[3] G. Klecak, H. Geleick, J. Frey, J. Soc. Cosmet. Chem. 28 (1977) 53.
[4] W.G. Larsen, Arch. Dermatol. 113 (1977) 623.
[5] H. Alenius, D.W. Roberts, Y. Tokura, A. Lauerma, G. Patlewicz, M.S. Roberts, Drug Discov. Today: Dis. Mech. 5 (2008) e211.
[6] M.D. Gober, A.A. Gaspari, Curr. Dir. Autoimmun. 10 (2008) 1.
[7] I. Kimber, D.A. Basketter, G.F. Gerberick, R.J. Dearman, Int. Immunopharmacol. 2 (2002) 201.
[8] F.D. Khan, S. Roychowdhury, A.A. Gaspari, C.K. Svensson, Expert Opin. Drug Metab. Toxicol. 2 (2006) 261.
[9] M. Divkovic, C.K. Pease, G.F. Gerberick, D.A. Basketter, Contact Dermatitis 53 (2005) 189.
[10] D.A. Basketter, A. Dooms-Goossens, A.T. Karlberg, J.P. Lepoittevin, Contact Dermatitis 32 (1995) 65.
[11] P. Aeby, T. Sieber, H. Beck, G.F. Gerberick, C.J. Goebel, J. Invest. Dermatol. 129 (2009) 99.
[12] A.S. Kalgutkar, I. Gardner, R.S. Obach, C.L. Shaffer, E. Callegari, K.R. Henne, A.E. Mutlib, D.K. Dalvie, J.S. Lee, Y. Nakai, J.P. O'Donnell, J. Boer, S.P. Harriman, Curr. Drug Metab. 6 (2005) 161.
[13] A.T. Karlberg, A. Dooms-Goossens, Contact Dermatitis 36 (1997) 201.
[14] D.J. Liberato, V.S. Byers, R.G. Dennick, N. Castagnoli Jr., J. Med. Chem. 24 (1981) 28.
[15] M. Skold, A. Borje, M. Matura, A.T. Karlberg, Contact Dermatitis 46 (2002) 267.
[16] J.M. Baron, D. Holler, R. Schiffer, S. Frankenberg, M. Neis, H.F. Merk, F.K. Jugert, J. Invest. Dermatol. 116 (2001) 541.
[17] M. Saeki, Y. Saito, M. Nagano, R. Teshima, S. Ozawa, J. Sawada, Int. Arch. Allergy Immunol. 127 (2002) 333.
[18] L.G. Yengi, Q. Xiang, J. Pan, J. Scatina, J. Kao, S.E. Ball, R. Fruncillo, G. Ferron, C. Roland Wolf, Anal. Biochem. 316 (2003) 103.
[19] C. Cheung, C.K. Smith, J.O. Hoog, S.A. Hotchkiss, Biochem. Biophys. Res. Commun. 261 (1999) 100.
[20] A. Janmohamed, C.T. Dolphin, I.R. Phillips, E.A. Shephard, Biochem. Pharmacol. 62 (2001) 777.
[21] M.D. Barratt, D.A. Basketter, Contact Dermatitis 27 (1992) 98.
[22] F. Bertrand, D.A. Basketter, D.W. Roberts, J.P. Lepoittevin, Chem. Res. Toxicol. 10 (1997) 335.
[23] D. Thompson, D. Constantin-Teodosiu, B. Egestad, H. Mickos, P. Moldeus, Biochem. Pharmacol. 39 (1990) 1587.
[24] A. Baumann, A. Faust, M.P. Law, M.T. Kuhlmann, K. Kopka, M. Schafers, U. Karst, Anal. Chem. 83 (2011) 5415.
[25] A. Baumann, W. Lohmann, T. Rose, K.C. Ahn, B.D. Hammock, U. Karst, N.H. Schebb, Drug. Metab. Dispos. 38 (2011) 2130.
[26] A. Baumann, W. Lohmann, B. Schubert, H. Oberacher, U. Karst, J. Chromatogr. A 1216 (2009) 3192.
[27] U. Jurva, H.V. Wikstrom, A.P. Bruins, Rapid Commun. Mass. Spectrom. 14 (2000) 529.
[28] W. Lohmann, R. Dötzer, G. Gutter, S.M. Van Leeuwen, U. Karst, J. Am. Soc. Mass Spectrom. 20 (2009) 138.
[29] T. Johansson, L. Weidolf, U. Jurva, Rapid Commun. Mass Spectrom. 21 (2007) 2323.
[30] W. Lohmann, U. Karst, Anal. Bioanal. Chem. 386 (2006) 1701.
[31] U. Jurva, A. Holmen, G. Gronberg, C. Masimirembwa, L. Weidolf, Chem. Res. Toxicol. 21 (2008) 928.
[32] A. Baumann, U. Karst, Expert Opin. Drug. Metab. Toxicol. 6 (2010) 715.
[33] W. Lohmann, U. Karst, Anal. Bioanal. Chem. 391 (2008) 79.
[34] E. Nouri-Nigjeh, R. Bischoff, A.P. Bruins, H.P. Permentier, Curr. Drug Metab. 12 (2010) 359.
[35] H.P. Permentier, A.P. Bruins, R. Bischoff, Mini Rev. Med. Chem. 8 (2008) 46.
[36] W. Lohmann, H. Hayen, U. Karst, Anal. Chem. 80 (2008) 9714.